CHAPTER 6

Fluorescence energy transfer kinetics of full-length

and truncated OmpA W7 mutants

6.1 INTRODUCTION

An ensemble of unfolded proteins theoretically should exhibit a broad, close to Gaussian, distribution of the end-to-end distances. This state is heterogeneous since there is a large number of degenerate conformations and high level of disorder in the configurations. As the polypeptide evolves from a given unfolded state to the folded, native state, the conformational freedom decreases and the configurational entropy becomes much lower than that of the unfolded protein. The energy landscape of a protein folding reaction resembles a funnel with many local minima (Figure 6.1) (Dobson et al., 1998). A long-term challenge of protein folding is understanding how a heterogeneous ensemble evolves to the uniformly folded, native state and determining at what stage the ensemble becomes homogeneous.

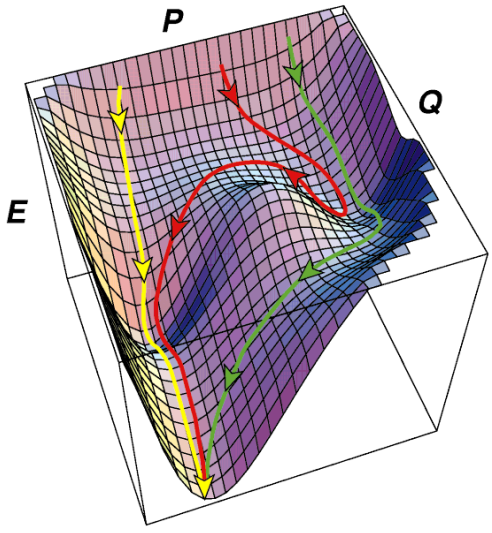

Figure 6.1. Sample potential energy landscape for lysozyme folding. Adapted from (Dobson et al., 1998).

Fluorescence energy transfer kinetics

Ensemble averaged fluorescence energy transfer (FET or FRET where R is resonance) does not provide information about conformational heterogeneity in the unfolded state or during the folding process. However, kinetics of FET will allow underlying distance distributions to be resolved and therefore provide information similar and complementary results to those obtained from single molecule studies (Fung & Stryer, 1978; Lakowicz et al., 1988; Navon et al., 2001; Lyubovitsky et al., 2002). An advantage of FET kinetics over single-molecule FET is that the system does not have to be immobilized on a surface. This avoids the problem of immobilization effects on the folded conformation or the folding rate of the protein. Low signal to noise ratios in single-molecule studies require the use of large dyes that give strong emission but may interfere with the folding process. Since signal is not an issue in ensemble measurements of FET kinetics, smaller and less disruptive dyes can be used.

Our group has done extensive studies on the development of fluorescence based probes to report on populations of unfolded, folded, and intermediate species as well as their conformational hetereogeneity for small, water-soluble proteins. FET kinetics have been shown to effectively monitor short and long-range interactions and conformational heterogeneity in the unfolded state and during the folding of dynamic polypeptides to the native state (Lyubovitsky et al., 2002; Lyubovitsky et al., 2002; Pletneva et al., 2005). This technique has been performed using yeast cytochrome *c* as a model protein since it has been extensively characterized (Moore, 1987; Lyubovitsky et al., 2002; Lyubovitsky et al., 2002). FET kinetics are powerful for providing probability distributions for the distance between a fluorescent donor (D) and an energy acceptor (A) of the folding

ensemble. Depending on the chosen probes, D-A distances as far as 100 Å can be studied.

Donor molecules will generally emit at wavelengths that overlap with the absorption of the acceptor molecules. When there is long-range dipole-dipole interaction between the emission energy of the donor (D) and the excitation energy of the acceptor (A), FET occurs through a singlet-singlet, nonradiative energy transfer process from the D to the A without emission or reabsorption of photons. The energy transfer rate depends on the distance between the D and A. Specifically it is inversely proportional to r^6. The Förster equation describes the energy transfer rate (k_{et}), which is dependent on the intrinsic decay rate of the D (k_o), the D-A distance (r), and the critical length or the Förster distance (r_o):

$$k_{et} = k_o\left(\frac{r_o}{r}\right)^6 . \qquad (1)$$

The rate constant will vary to the sixth power of the ratio of the critical length to the D-A distance. The critical length depends on the D and A spectroscopic and photophysical properties as well as the refractive index of the D-A environment:

$$r_o^{\,6} = 8.79\times10^{-5}\,\frac{\mathrm{K}^2\Phi_D J}{n^4} . \qquad (2)$$

Here, the dipole orientation factor, κ^2, describes the relative orientation of the D-A dipole. If the D and A freely rotate, κ^2 is 2/3. Φ_D is the D fluorescence quantum yield in the absence of A and n is the refractive index. The overlap integral, J, of the D fluorescence and A absorption is given by

$$J = \int \varepsilon_A(\lambda) F_D(\lambda) \lambda^4 d\lambda \ \ \mathrm{cm^3\,M^{-1}}, \qquad (3)$$

where λ is the wavelength (nm), F_D is the normalized D fluorescence emission spectrum, and ε_A is the A absorption spectrum ($M^{-1}cm^{-1}$).

The critical length defines the range of distances that can be evaluated, specifically $0.3r_o < r < 1.5\ r_o$. It is the distance where 50 % FET efficiency occurs, which means that when *r* is equal to r_o, half of the D molecules decay by energy transfer and the other half decay by regular radiative and non-radiative processes (i.e., k_{et} is equal to k_o when D-A distance is equal to r_o).

The distance distribution between the D and A in a protein can be calculated from FET kinetics (Figure 6.2). In the unfolded state, the ensemble of proteins will be heterogeneous with a broad distribution of D-A distances (*P(r)*). The value of the average *r* will increase with the number of amino acids in a protein. A distribution of fluorescence decays rates (*P(k)*) results and the fluorescence decays (*I(t)*) are nonexponential. As the protein folds to the native state, the ensemble becomes more homogeneous, resulting in a more narrow range of *P(r)*, shorter *r*, and faster decay rates.

Starting from the fluorescence decay kinetics, which we experimentally measure, we can obtain *P(k)* by inverting the discrete Laplace transform that describes *I(t)* using the equation:

$$I(t) = \sum_{k=ko}^{\infty} P(k)e^{-kt} \ . \qquad (4)$$

The Förster equation is then used to transform *P(k)* to *P(r)*.

FET kinetics have the potential to study the dynamics of the self-assembly of OmpA into lipid bilayers and provide new insights into the mechanism of β-barrel membrane protein folding. OmpA is an ideal integral membrane protein model for FET kinetics since much is known about the folding timescales and kinetic intermediates

(Kleinschmidt et al., 1999; Kleinschmidt & Tamm, 1999; Tamm et al., 2001). Studies with time-resolved distance determination by fluorescence quenching (TDFQ) experiments, as described in section 5.1, are informative but are still an ensemble averaged technique since only the steady-state fluorescence are collected. FET kinetics will provide information on the heterogeneity and D-A distances of OmpA intermediates.

OmpA has been labeled with a dansyl fluorophore as an energy acceptor from a W7 donor. Both the full-length and truncated variants, W7/A175C-Dns and W7t/A175C-Dns, have been successfully prepared. FET kinetics were used to investigate the refolding ensemble of these two systems under conditions promoting (30 ^{o}C) and discouraging insertion (15 ^{o}C) into DMPC vesicles.

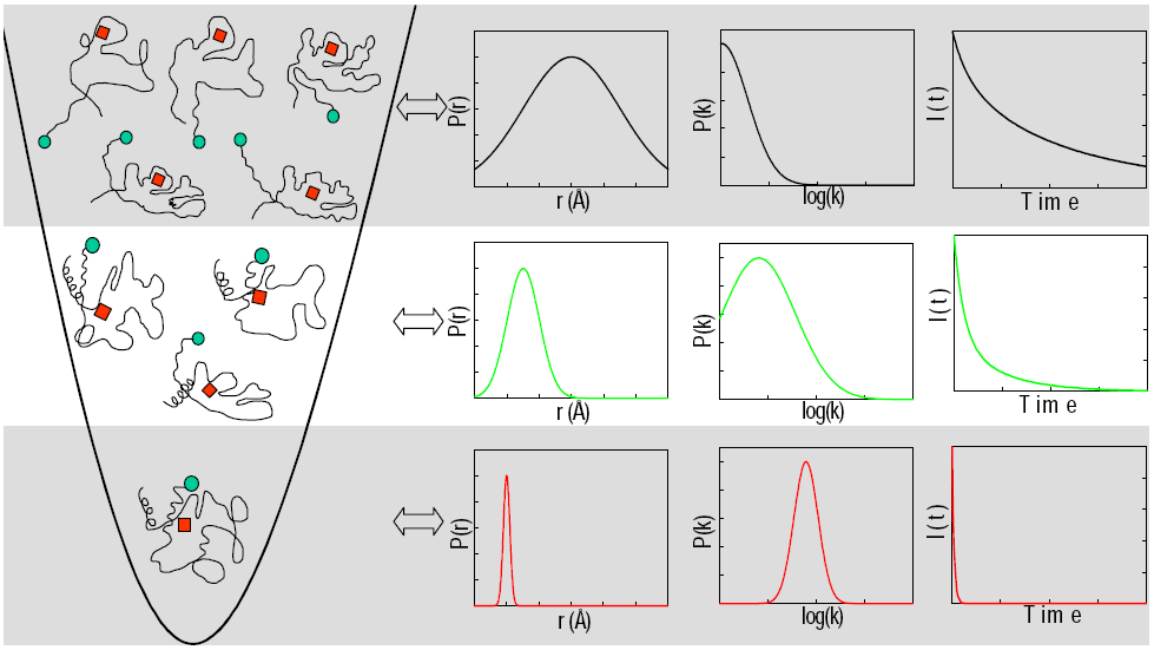

Figure 6.2. Schematic depicting the relationship between protein conformations and fluorescence decay kinetics. The left side shows a simplified energy landscape funnel. At the top of the funnel, an ensemble of unfolded proteins will exhibit a broad distribution of distances ($P(r)$) between the FET donors and acceptors and slow excited-decay kinetics. At the bottom, an ensemble of folded proteins will exhibit a narrow distance distribution and faster excited-state decay kinetics. The distance distribution function can be transformed using Eq. 1 to a distribution of fluorescence decay rates (k). P(k) can be transformed using Eq. 4 to a fluorescence decay intensity profile ($I(t)$) . Figure obtained from Julia Lyubovitsky's dissertation (Lyubovitsky, 2003).

6.2 EXPERIMENTALS

Dansyl-labeling of W7/A175C and W7t/A175C

A solution of ~90 μM protein with 10-fold molar TCEP (Tris(2-carboxyethyl)phosphine) in 8 M urea, 20 mM KPi, pH 7.3 was stirred under argon in a small round bottom flask for ~1 hr with periodic vacuum pumping. A concentrated solution of 5-((((2-iodoacetyl)amino)ethyl)amino)-naphthalene-1-sulfonic acid (1,5-IEADANS) label was prepared in DMSO. Under a flow of argon, the label was added to the protein solution to a final concentration of 10 times the protein concentration. The flask was resealed and deoxygenated with vacuum/argon cycles several times. The reaction proceeded for 5 hours under argon atmosphere and in the dark to minimize photochemical side reactions, followed by reaction quenching with excess dithiothreitol (DTT). Free dye was removed either by dialysis overnight into 4 M urea, 0.5% 2-mercaptoethanol, 15 mM Tris, pH 8.5 or by desalting using a PD-10 column (Amersham Biosciences).

In determining the ideal labeling conditions, control experiments were performed to determine the minimum time needed for labeling. Side by side dansyl (Dns) labeling reactions of W7/A175C and W7/CS/CS were carried out and aliquots at various time points were removed and quenched with DTT. The aliquots were desalted and free dye was removed using Micro Bio-Spin columns (BioRad)**.** Protein aliquots were concentrated in Microcon Centrifugal Filter Devices (Millipore) with 10,000 molecular weight cut off (MWCO). UV-visible absorption spectra were then recorded for each time point and the molar ratio between D and A were calculated to determine the time when the labeling reaction should be quenched.

Purification of Dns-labeled protein

Purification of the Dns-protein was performed in the dark under red light using FPLC protocols described in Chapter 2. UV-visible absorption was used to determine which purified fractions to combine. Purified protein was then concentrated using Amicon stirred cells with MWCO of 10 kDa and 3 kDa for full-length and truncated proteins, respectively. Concentrated protein was stored in the dark, covered with foil, in 4^{o} C and used for measurements within 1 week of purification.

Tryptic mapping of labeled sites

To verify that the cysteine at position 175 is the site of labeling, Dns-protein samples were submitted to the Caltech Protein and Peptide Microanalytical Lab for peptide mapping of the tryptic digested product. Dns-proteins were run on SDS-PAGE and protein bands were cut out from the gels. Samples were submitted for in-gel trypsin digestion and mass spectrometry by matrix-assisted laser desorption/ionization-time of flight (MALDI-TOF).

CD and SSFl measurements

CD for the labeled protein was measured as described in Chapter 3. Steady-state fluorescence scans over the 2 hr course of folding were measured at 30 ^{o}C as described in Chapter 4. Dns emission spectra were collected over a 2 hr period using 340 nm for excitation.

Measurement of Dns excited-state lifetimes

The synthesis and purification of the Dns-cysteine model complex were adapted from published protocols (Lyubovitsky et al., 2002) by Melanie A. Pribisko. Control measurements of the excited-state decay for this model complex (~3 μM) in urea, buffer,

micelles, and vesicles were collected at 30 ^{o}C and 15 ^{o}C. A thermocouple was used to ensure that the sample temperatures were close to the desired values. Dns excited-state lifetimes from Dns-protein (~3 μM) were also collected at the two temperatures when unfolded in urea and buffer and folded in micelles and vesicles.

Dns was excited using the third harmonic of a picosecond Nd:YAG laser (Spectra-physics) at 355 nm (76 MHz, ≤ 5 mW power) and the emission was detected at 90^{o} to excitation beam using a picosecond streak camera (Hamamatsu C5680). Magic-angle conditions were used in the measurements. Dns fluorescence was selected with a 420 nm long pass filter (LPF). The streak camera was used in photon counting mode.

FET kinetics

Dns-protein was excited at 292 nm and Trp lifetimes were collected as described in Chapter 3 over a period of 6 hours after the folding reaction was initiated by the manual syringe injection of Dns-protein into either micelles or vesicles equilibrated at 30 ^{o}C or 15 ^{o}C. Trp emission was selected as described previously in Chapter 3. Dns emission with 292 nm excitation was collected using a 475 nm LPF. When data was not actively being collected, Dns-protein was either placed in a 35^{o} C oven or into the 15^{o} C water bath/circulator to maintain temperature. The excitation power at the sample was ~350-400 μW and the acquisition time was ~4 min. Trp lifetimes were also measured for Dns-protein in urea and buffer. UV-visible absorption spectra were collected after each measurement to determine protein concentration.

Control measurements of W7/A175C and W7t/A175C under the unfolded (urea, buffer) and folded (micelles, vesicles) conditions were collected during the time course of

folding at approximately the same time points as the measurements collected for the Dns-protein.

Data analysis

Dns lifetimes were fitted to biexponential fits using the program Igor Pro (Wavemetrics). Energy transfer rates (k_{et}) were obtained using a deconvolution program that basically obtains the ratio of quenched to unquenched excited-state decays. The unquenched excited-state decays were measured from W7/A175C and W7t/A175C. A MATLAB algorithm (LSQNONNEG) that minimizes the sum of the squared deviations (X^2) between observed and calculated *I(t)*, subjected to a nonnegativity constraint, P(k) ≥ 0 ($\forall$ k) was used to fit the energy transfer rates. Results produced the probability distribution for the rate constants. The Förster equation (Eq. 1) was used to convert rate constants to distances.

3.3 RESULTS AND DISCUSSION

Protein derivatization with dansyl

We have chosen to use tryptophan (Trp) and dansyl (Dns) as the FET donor and acceptor, respectively (Figure 6.3). Trp has been extensively used as an energy transfer probe (Royer, 2006; Kimura et al., 2007). OmpA contains 5 native Trp, which can serve as native donors in our studies. FET pairs ideally should be structurally small to minimize interference with folding energetics and dynamics. Dns is a small fluorophore with a MW of ~400 and should not interfere drastically with the folding of a full-length 35 kDa or truncated 19 kDa OmpA protein. The critical distance for the Trp-Dns pair

was experimentally measured to be 21 Å using NATA and N-acetyl-cysteine-Dns as the D-A models. This r_o value is consistent with the literature (Wu & Brand, 1994).

A single cysteine residue was introduced at position 175 in W7 and W7t for derivatization with Dns, a thiol-reactive dye (Figure 6.4). The α-carbon distance from position 7 to 175 is ~16 Å (Figure 6.5). The labeling reaction was performed on unfolded OmpA in 8 M urea, which presumably would facilitate the rate of folding. The addition of excess TCEP to the labeling reaction was used to prevent formation of intermolecular disulfide bonds. Dialysis with 4 M urea was used instead of 8 M urea because this amount should be enough to solubilize the protein and yet not waste urea. Removal of excess dye and DTT was better achieved through dialysis rather than desalting.

Experiments were initially carried out to determine the time necessary for labeling OmpA with Dns (Figure 6.6). The ratio of Dns to protein concentration was determined for each reaction time point and revealed that 5 hr was sufficient for 1:1 Dns labeling of the protein. The unfolded state of OmpA facilitates the labeling reaction. Even at 33 hr, reaction of Dns with the Cys-less W7/C290S/C302S did not mislabel other amino acids, as evidenced by the absence of a Dns peak at 336 nm in the absorption spectrum.

Tryptic digest and MALDI-TOF

The resulting masses of the peptide fragments from the trypsin digest revealed that A175C was labeled with Dns since masses of fragments matched those of the calculated masses.

Measurement of Dns lifetimes

The lifetime and amplitudes from biexponential fits of Dns excited-state lifetimes are listed in Table 6.1.

Steady-state fluorescence

Steady-state fluorescence scans over the course of folding for W7/A175C-Dns and W7t/A175C-Dns are shown in Figures 6.7 and 6.8. These scans seem to suggest that energy transfer from Trp to Dns occurs throughout the entire 2 hr folding period since the Dns emission continues to rise. This rise is not seen with direct 340 nm excitation of Dns (Figure 6.9), thus indicating that the rise is due to the Trp. Data analysis of the refolding scans was done by plotting the emission maxima and integrated intensities against folding time. On a closer inspection of the traces, we see that the maximum intensity of the Trp emission is steady for the first 25 min for W7/A175C-Dns and 40 min for W7t/A175C. This period of steady intensity is not characteristic of the unlabeled protein as shown in Figures 6.10 and 6.11, where the maximum intensity increases at the start of protein folding. Therefore, the steady intensity that is observed with the Dns-protein is due to energy transfer from the Trp to Dns. The continued rise in Dns after 25-40 min is not due to energy transfer but due to excitation of the Dns arising from the increase in Trp lifetime as the protein folds into the bilayer.

FET kinetics

Trp excited state decays from W7/A175C-Dns and W7/A175C-Dns were acquired as well as the Dns emission with 290 nm excitation. Typical data sets are shown in Figure 6.12. Since the distance for W7 and A175C-Dns is ~16 Å, well within the measurable range of energy transfer, we were surprised to see that Trp decay rates do not increase as the protein folds into the native structure. At first, the absence of Trp quenching seems to contradict the slow rise seen in the Dns emission from W7/A175C-Dns, which we assigned to energy transfer. Biexponential fits of the Dns emission

revealed that the energy transfer rates to Dns were similar to rates of the Trp decays. Therefore, the increase in Trp lifetime upon folding offsets the energy transfer rates.

Control lifetime measurements using W7/A175C and W7t/A175C without Dns were measured at approximately the same time points as the Dns-protein measurements. These unquenched lifetimes were used to "deconvolute" and remove the increase in Trp lifetime from the FET kinetics data, resulting in energy transfer rates. These rates were then fit to the LSQNONNEG Matlab program to obtain the probability distributions of rate constants.

Tables 6.2 – 6.9 summarize the probability weighted energy transfer rates (k_{et}) and the D-A distances (r). Lifetime data acquired from 20 s to 4 min of folding into DMPC resulted in D-A distances of ~24 Å. Within ~15 min, FET kinetics revealed that the D-A sites are already at native distances of 18-20 Å and do not change over the course of ~6 hr. Therefore, the barrel ends are associated early in the folding process. Also, ~20-30 % of the population remains unquenched, which may correspond to the unfolded population that was observed by Surrey and Jahnig. Figure 6.13 shows the ratio of unquenched to quenched data. It is clearly seen that by 14 min, W7/A175C-Dns energy transfer to Dns is complete and remains constant since no further changes in rate constants and distances are observed. For W7t/A175C-Dns, this energy transfer is done between 10-60 min. We did not observe energy transfer for the W7/A175C-Dns and W7t/A175C-Dns unfolded in urea and buffer. This species is likely different from the adsorbed species since no definite secondary structures were observed in the CD and SSFl spectra. It is also not the same species as the one that folds to the native structure at

30 ^{o}C since no energy transfer is observed. Thus, this indicates that another OmpA species may exist in urea and buffer.

The FET kinetics data revealed that at 15 ^{o}C in DMPC, most of the protein (~90 %) does not develop native distances for the W7 and A175C-Dns sites. Based on this lack of FET from the D to the A, and along with CD and fluorescence data from Chapter 5, we conclude that the 15 ^{o}C adsorbed species is not a true intermediate of the folding pathway.

A simple, possible model, would be that the pathway to arrive at the adsorbed species is more smooth and less rugged that the pathway to arrive at the native structure, which occurs in a few hours. When the pathway to the native structure is shut off by the low temperature, gel phase of the lipid vesicles, the proteins immediately move along some low barrier pathway to the adsorbed species. Conversion of some adsorbed species to the native state is possible when the temperature is raised above the lipid gel-liquid transition temperature (Surrey & Jahnig, 1992). Indeed, we also observed that the rate constants are similar to those at 30 ^{o}C after raising the temperature from 15 ^{o}C.

It was also observed that folding into OG micelles is not as efficient as folding into DMPC vesicles. In the micelle environment, ~45-53 % unquenched population exists for the full-length W7A175C-Dns and ~76-80 % exists for the truncated form, W7t/A175C-Dns. Refolding into cold OG micelles (15^{o}C) is possible but is not as efficient (60-70 % unquenched) as folding into micelles at higher temperatures (45-53 % unquenched).

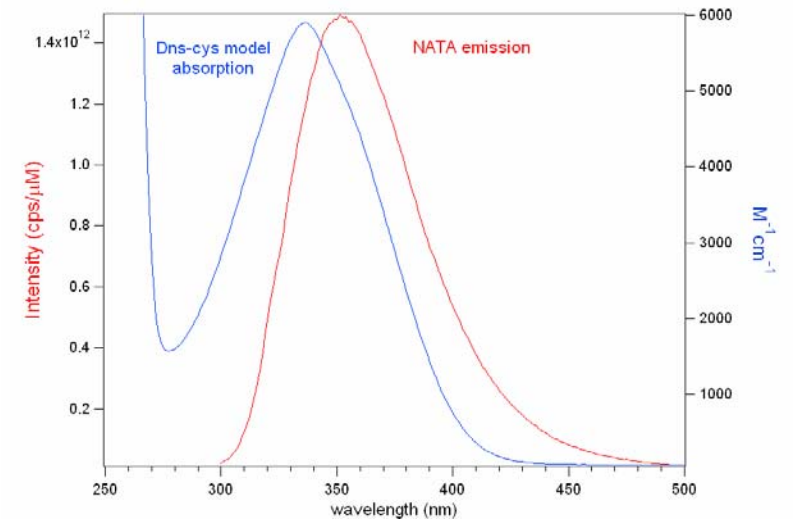

Figure 6.3. Overlap of NATA emission with normalized Dns absorption.

Sample, environment	30°C lifetimes (ns), (% amplitude)	15°C lifetimes (ns), (% amplitude)
Dns-cys, urea	13.8 (91%), 1.8 (9%)	13.2 (90%), 1.3 (10%)
Dns-cys, KPi	11.7 (92%), 1.9 (8%)	11.4 (92%), 1.5 (8%)
DNS-cys, OG	11.8 (90%), 1.9 (10%)	11.4 (89%), 2.0 (11%)
DNS-cys, DMPC	11.7 (92%), 2.0 ns (8%)	11.2 (91%), 1.4 (9%)
W7-Dns, urea	18.0 (67%), 12.3 (33%)	15 (91%), 1.5 (9%)
W7-Dns, KPi	20.5 (71%), 11.2 (29%)	16.8 (92%), 1.5 (8%)
W7-Dns, OG	20.9 (70%), 10.1 (30%)	16.9 (89%), 1.7 (11%)
W7-Dns, DMPC	17.9(91%), 1.8 (9%)	25.3 (81%), 5.7 (19%)
W7t-Dns, urea	14.9 (89%), 1.9 (11%)	14.4 (90%), 1.6 (10%)
W7t-Dns, KPI	15.2 (89%), 1.6 (11%)	14.7 (90%), 1.7 (10%)
W7t-Dns, OG	15.0 (88%) , 2.0 (12%)	15.3 (86%) , 1.5 (14%)
W7t-Dns, DMPC	15.3 (87%), 2.0 (13%)	20 (88%), 1.5 (12%)

Table 6.1. Lifetimes and amplitudes of the Dns excited-state decay

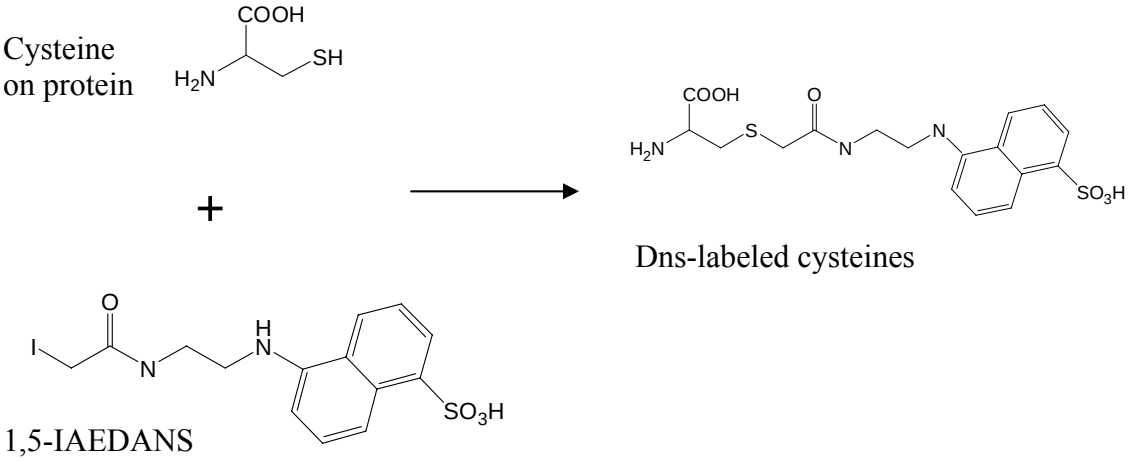

Figure 6.4. Reaction of a general cysteine with 1,5 IEADANS to produce the dansylated cysteine on the protein. Note that cysteine was drawn as a free amino acid for simplicity. In reality, these cysteines are attached to the protein.

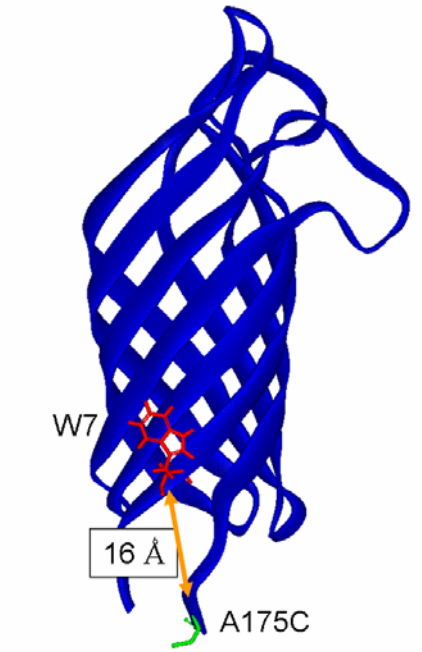

Figure 6.5. Structure of OmpA showing the positions and distance of W7 and A175C. The α-carbon position of W7 is 16 Å from to A175C, according to the NMR structure (PDB file IG90).

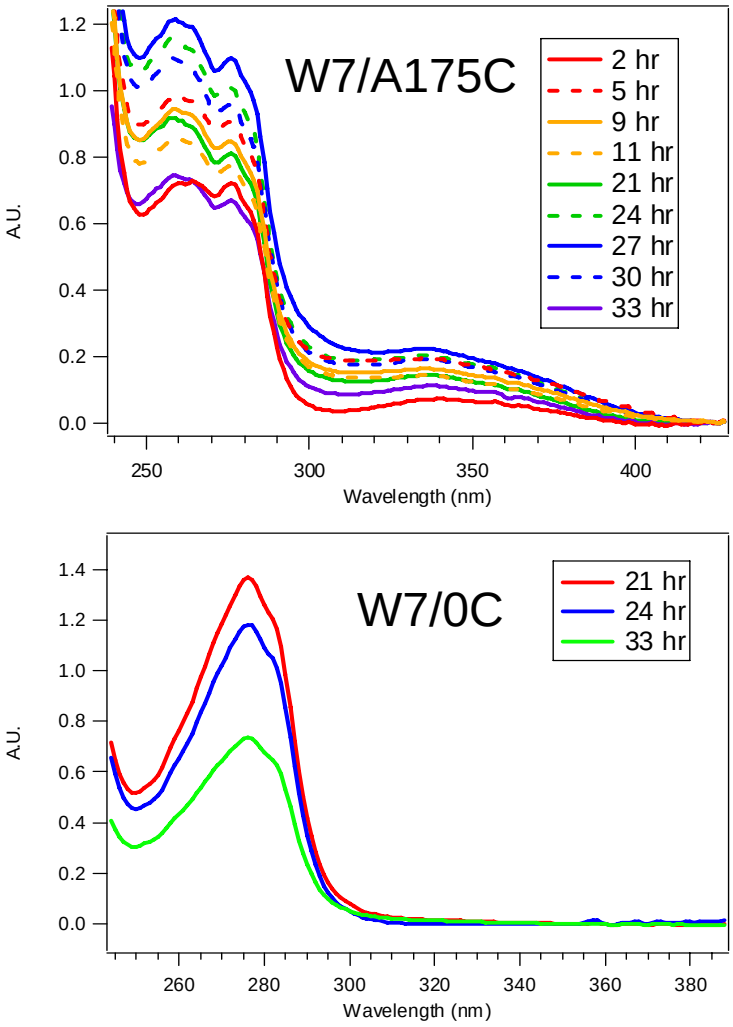

Hours after addition of IAEDANS	[Dns]/[protein]
2	0.62
5	1.39
9	1.25
11	1.19
21	1.15
24	1.31
27	1.30
30	1.30
33	1.08

Figure 6.6. Absorption spectra of time points from a side-by-side labeling reaction of W7/A175C and the control protein, W7/C290S/C302S (abbreviated as W7/0C), with IAEDANS. The ratio of Dns to protein indicates that 5 hr is sufficient for labeling.

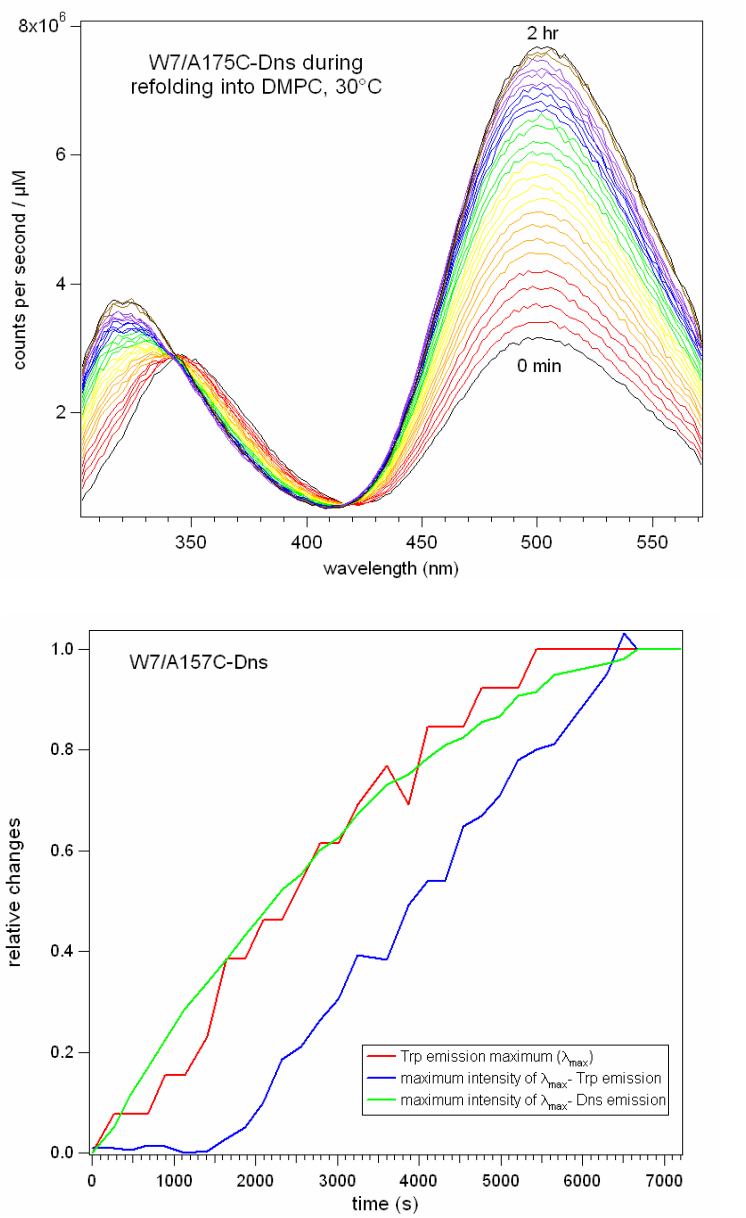

Figure 6.7. Fluorescence spectra of full-length W7/A175C-Dns immediately following protein injection to initiate folding into DMPC vesicles at 30 ^{o}C. Two general processes are observed (top): blue-shift in emission maxima and quantum yield increase. Relative changes in emission maxima (bottom, blue trace) and emission intensity (bottom, green and red traces) are shown as a function of folding time. Traces were normalized so that a value of "1" corresponds to the emission maximum or intensity at t = 2 hr.

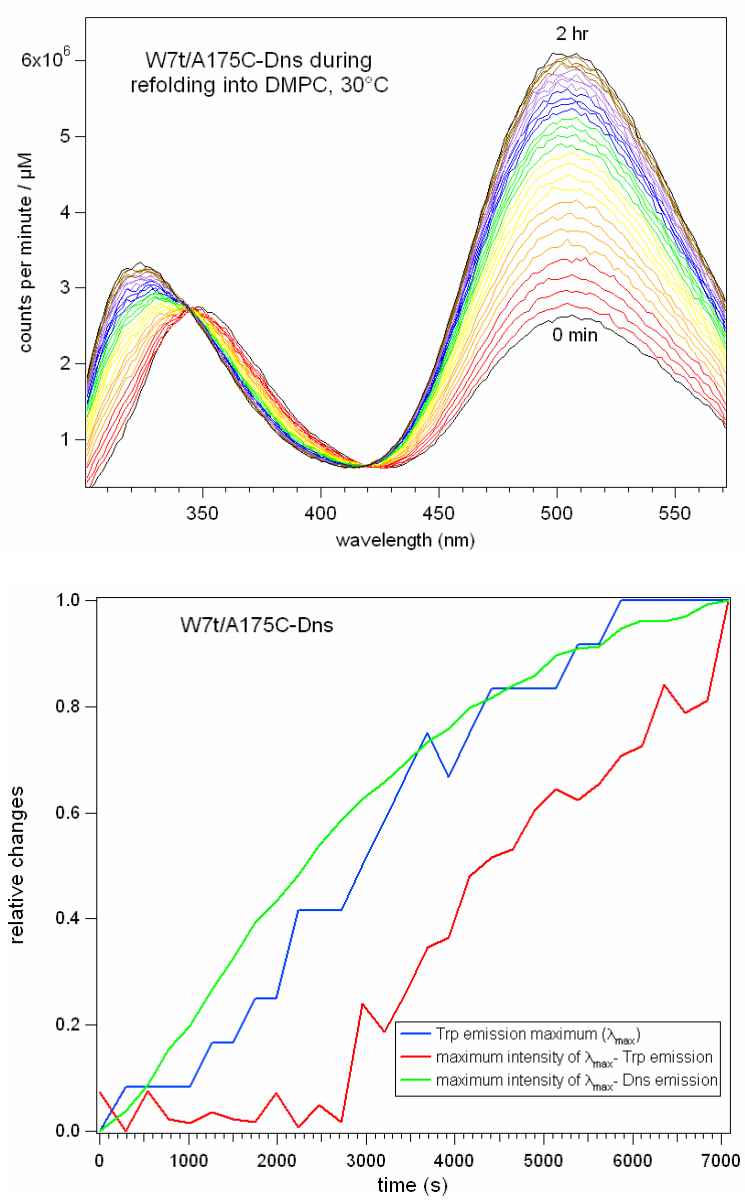

Figure 6.8. Fluorescence spectra of truncated W7t/A175C-Dns immediately following protein injection to initiate folding into DMPC vesicles at 30 ^{o}C. Two general processes are observed (top): blue-shift in emission maxima and quantum yield increase. Relative changes in emission maxima (bottom, blue trace) and emission intensity (bottom, green and red traces) are shown as a function of folding time. Traces were normalized so that a value of "1" corresponds to the emission maximum or intensity at t = 2 hr.

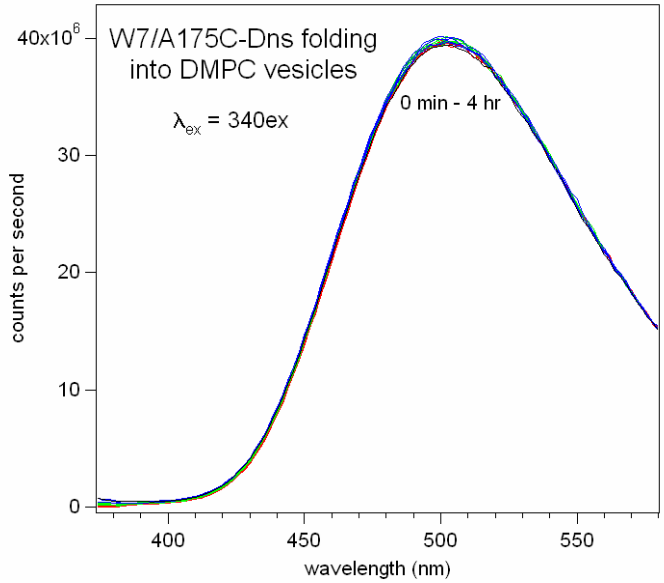

Figure 6.9. Excitation of Dns in W7/A175C-Dns with 340 nm excitation over the course of 4 hr does not produce a continuous rise in emission.

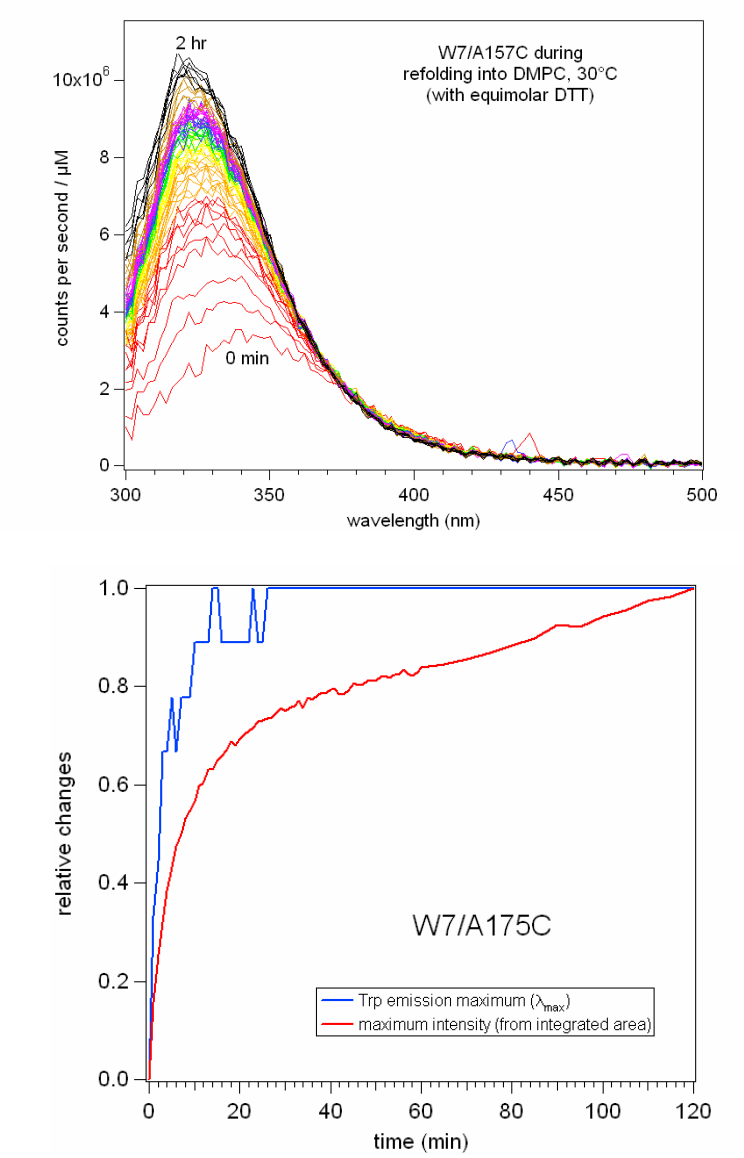

Figure 6.10. Fluorescence spectra of W7/A175C (unlabeled) immediately following protein injection to initiate folding into DMPC vesicles at 30 °C. Relative changes in emission maxima (bottom, blue trace) and emission intensity (bottom, red trace) are shown as a function of folding time. Traces were normalized so that a value of "1" corresponds to the emission maximum or intensity at t = 2 hr.

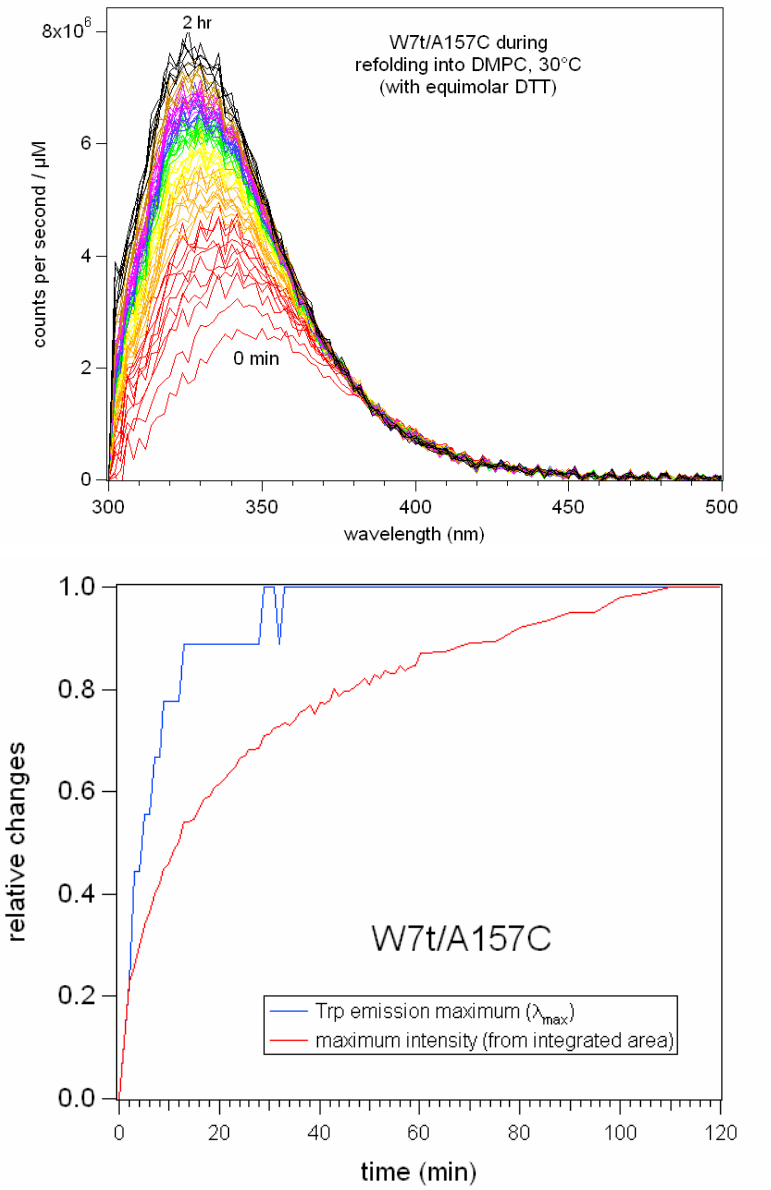

Figure 6.11. Fluorescence spectra of W7t/A175C (unlabeled) immediately following protein injection to initiate folding into DMPC vesicles at 30°C. Relative changes in emission maxima (bottom, blue trace) and emission intensity (bottom, red trace) are shown as a function of folding time. Traces were normalized so that a value of "1" corresponds to the emission maximum or intensity at t = 2 hr.

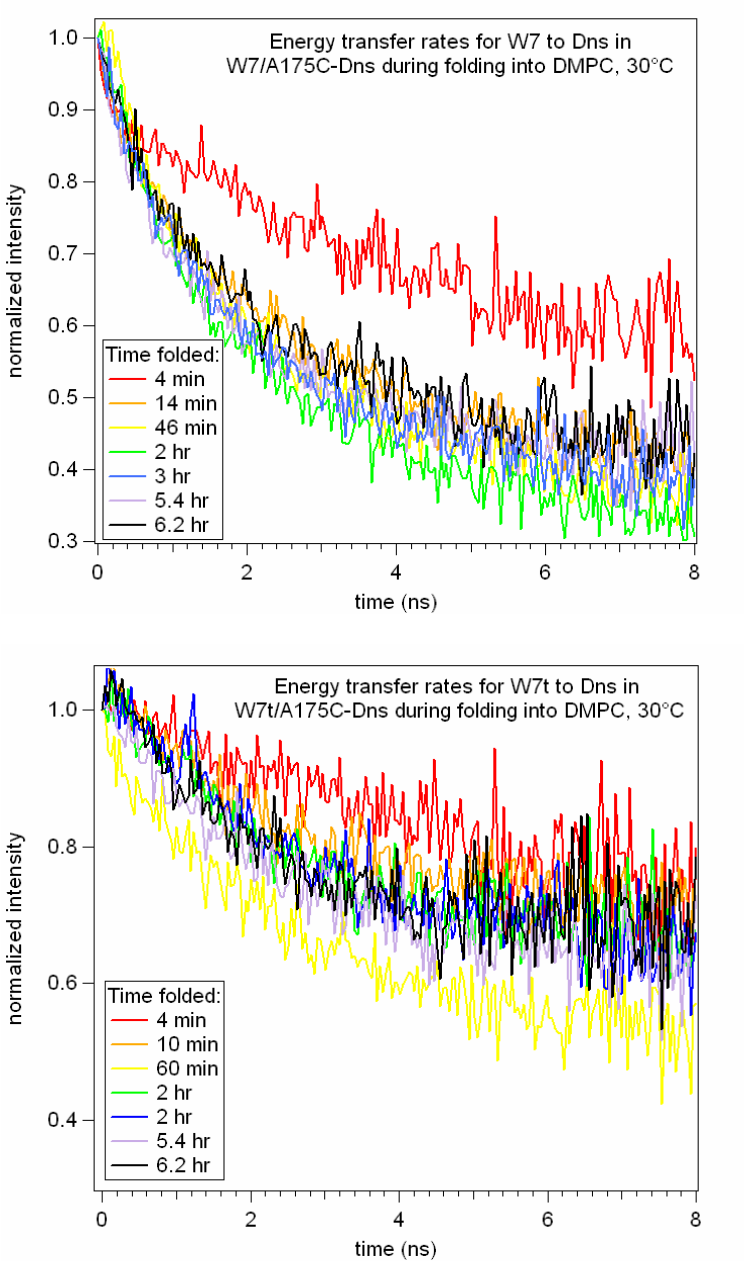

Figure 6. 12. Energy transfer rates are shown for the different folding times for W7/A175C-Dns and W7t/A175C-Dns. The energy transfer rate has decayed to a constant rate by ~14 min for W7/A175C and between 10-60 min for W7t/A175C.

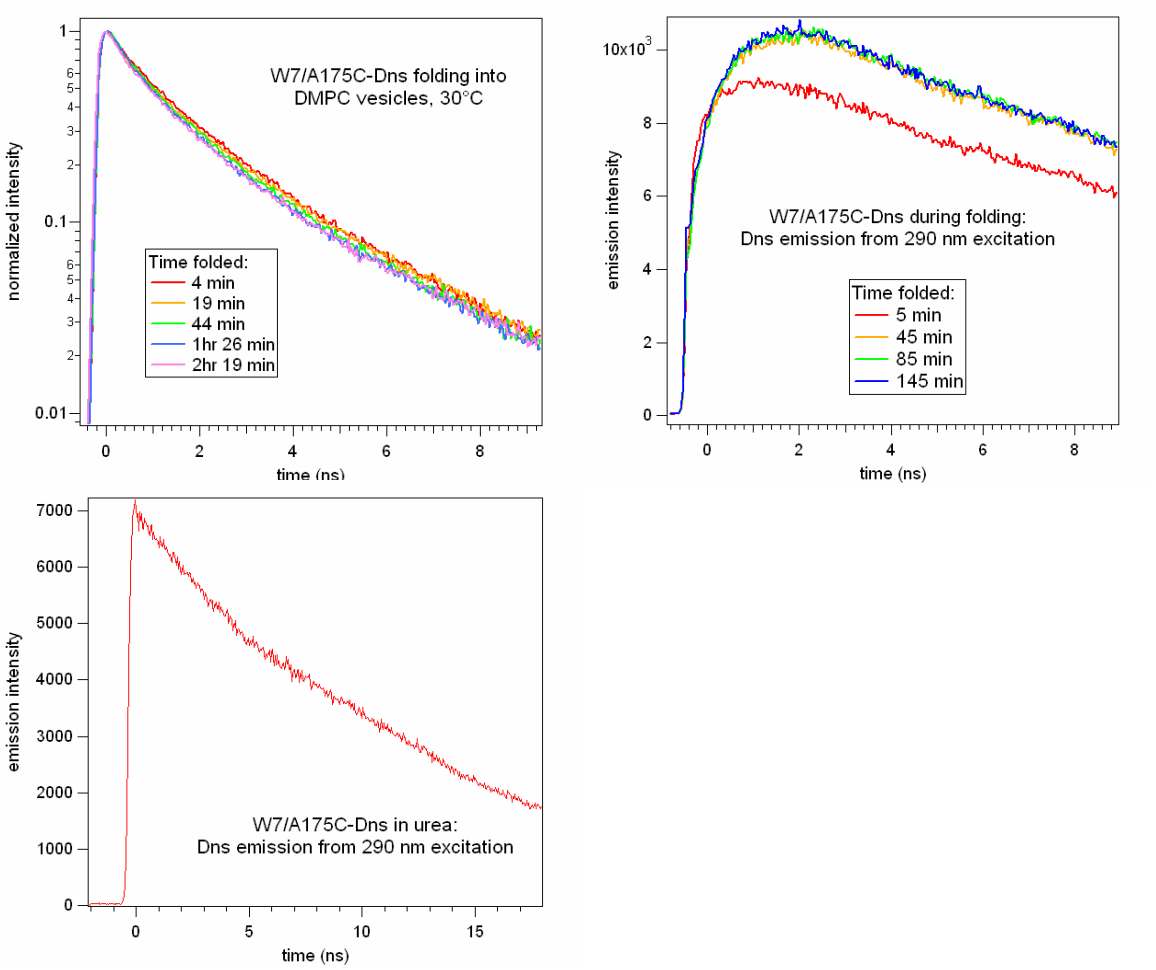

Figure 6. 13. Typical data sets collected for FET kinetics. Top, left graph are measurements of Trp decays as the protein folds into DMPC vesicles; Trp decays become only slightly faster as the protein folds. Top, right graph are measurements of Dns emission using 290 nm excitation; energy transfer is observed as a slow rise in intensity. Bottom graph is Dns emission from W7/A175C-Dns in urea; no energy transfer to Dns is observed.

Time folded	Weighted k_{et} (1/ns)	Weighted r (Å)	Unquenched (%)
4 min	0.09	24	30
14 min	0.66	20	37
46 min	0.80	18	54
2 hr	0.58	20	22
3 hr	0.65	19	36
5.4 hr	0.84	19	39
6.2 hr	0.63	20	38

Table 6.2. W7/A175C folding into DMPC vesicles at 30 ^{o}C. Probability weighted energy transfer rates (k_{et}) and their corresponding weighted distances (r). The percent of unquenched fluorescence is also listed.

Time folded	Unquenched (%)
4 min	87
14 min	92
36 min	93
1.2 hr	91
2 hr	88
2.8 hr	82

Table 6.3. Percentage of unquenched Trp fluorescence for W7/A175C folding into DMPC vesicles at 15 ^{o}C.

Time folded	Weighted *k* (1/ns)	Weighted *r* (Å)	% unquenched
4 min	0.11	25	54
14 min	0.35	21	68
46 min	0.53	20	49
2 hr	0.21	21	63
3 hr	0.38	21	60
5.4 hr	0.46	20	65
6.2 hr	0.47	20	66

Table 6.4. W7t/A175C folding into DMPC vesicles at 30 ^{o}C. Probability weighted energy transfer rates (k_{et}) and their corresponding weighted distances (r). The percent of unquenched fluorescence is also listed.

Time folded	Unquenched (%)
4 min	89
14 min	91
36 min	90
1.2 hr	94
2 hr	94
2.8 hr	96

Table 6.5. Percentage of unquenched Trp fluorescence for W7t/A175C folding into DMPC vesicles at 15 ^{o}C.

Time folded	Weighted *k* (1/ns)	Weighted *r* (Å)	% unquenched
4 min	0.84	18	53
12 min	0.19	18	45
56 min	1.2	17	48
1.9 hr	1.0	18	44
4.6 hr	0.10	18	48

Table 6.6. W7/A175C folding into OG micelles at 30 ^{o}C. Probability weighted energy transfer rates (k_{et}) and their corresponding weighted distances (r). The percent of unquenched fluorescence is also listed.

Time folded	Weighted *k* (1/ns)	Weighted *r* (Å)	% unquenched
4 min	1.1	18	71
16 min	0.98	18	61
58 min	1.3	17	60

Table 6.7. W7/A175C folding into OG micelles at 15 ^{o}C. Probability weighted energy transfer rates (k_{et}) and their corresponding weighted distances (r). The percent of unquenched fluorescence is also listed.

Time folded	Weighted *k* (1/ns)	Weighted *r* (Å)	% unquenched
4 min	1.3	17	77
13 min	2.3	15	77
1.1 hr	1.5	16	76
2.4 hr	1.4	16	77
4.4 hr	1.2	17	80

Table 6.8. W7t/A175C folding into OG micelles at 30°C. Probability weighted energy transfer rates (k_{et}) and their corresponding weighted distances (r). The percent of unquenched fluorescence is also listed.

Time folded	Weighted *k* (1/ns)	Weighted *r* (Å)	% unquenched
4 min	1.2	18	73
14 min	1.3	17	66
54 min	1.6	17	65

Table 6.9. W7t/A175C folding into OG micelles at 15°C. Probability weighted energy transfer rates (k_{et}) and their corresponding weighted distances (r). The percent of unquenched fluorescence is also listed.

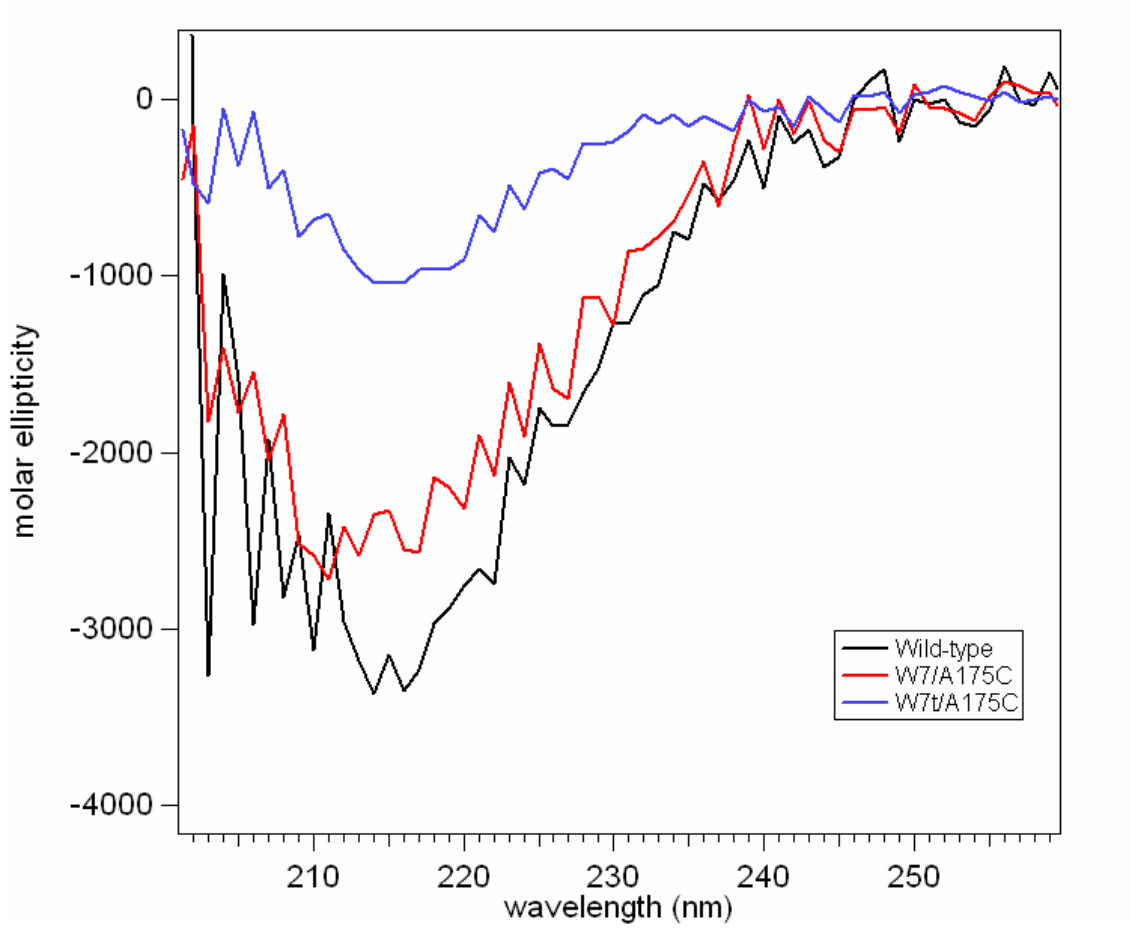

Figure 6.14. CD spectra of W7/A175C, W7t/A175C, and wild-type OmpA. Note that the ellipticities are lower than those from Chapter 3, most likely due to inaccurate protein concentrations used to determine molar ellipticities.

6.4 CONCLUSIONS

The experiments described in this chapter are the first to use fluorescence energy transfer kinetics to investigate the refolding of an integral membrane protein. A dansyl fluorophore has been used to label a mutant cysteine residue 175 in both full-length and truncated OmpA forms of the single-tryptophan variants. We have successfully measured rates of fluorescence energy transfer from tryptophan to dansyl as the polypeptide folds and inserts into micelles and lipid bilayers at temperatures above and below the lipid gel-liquid phase temperature. These studies provide new evidence that the barrel ends associate with native distances within the first 15 minutes of folding rather than towards the end of folding. It is ambiguous whether the adsorbed species is an on-pathway folding intermediate. Our measurements showed that virtually no energy transfer occurs from tryptophan to dansyl when the protein is in this adsorbed state, thus providing strong evidence that this species is not a true intermediate in the folding pathway. For tryptophan at position 7, it appears that the truncated form labeled with Dns does not fold as efficiently as the full-length form. Better folding efficiency is also observed with lipid vesicles than with detergent micelles. These studies show that FET kinetics are a powerful method for gaining mechanistic insight into membrane protein folding.

6.5 REFERENCES

Dobson, C. M., Sali, A., and Karplus, M. (1998) Protein folding: A perspective from theory and experiment, *Angewandte Chemie-International Edition 37*, 868-893.

Fung, B. K. K., and Stryer, L. (1978) Surface density determination in membranes by fluorescence energy-transfer, *Biochemistry 17*, 5241-5248.

Kimura, T., Lee, J. C., Gray, H. B., and Winkler, J. R. (2007) Site-specific collapse dynamics guide the formation of the cytochrome c ' four-helix bundle, *Proceedings of the National Academy of Sciences of the United States of America 104*, 117-122.

Kleinschmidt, J. H., den Blaauwen, T., Driessen, A. J. M., and Tamm, L. K. (1999) Outer membrane protein A of Escherichia coli inserts and folds into lipid bilayers by a concerted mechanism, *Biochemistry 38*, 5006-5016.

Kleinschmidt, J. H., and Tamm, L. K. (1999) Time-resolved distance determination by tryptophan fluorescence quenching: Probing intermediates in membrane protein folding, *Biochemistry 38*, 4996-5005.

Lakowicz, J. R., Gryczynski, I., Cheung, H. C., Wang, C. K., Johnson, M. L., and Joshi, N. (1988) Distance distributions in protein recovered by using frequency - domain fluorometery - applications to troponin-I and its complex with troponin-c, *Biochemistry 27*, 9149-9160.

Lyubovitsky, J. G., Gray, H. B., and Winkler, J. R. (2002) Mapping the cytochrome c folding landscape, *Journal of the American Chemical Society 124*, 5481-5485.

Lyubovitsky, J. G., Gray, H. B., and Winkler, J. R. (2002) Structural features of the cytochrome c molten globule revealed by fluorescence energy transfer kinetics, *Journal of the American Chemical Society 124*, 14840-14841.

Lyubovitsky, J. G. (2003) Mapping the cytochrome *c* folding landscape, in *Department of Chemistry*, California Institute of Technology, Pasadena, CA.

Moore, G. R., Pettigrew, G.W. (1987) *Cytochromes c: Biological Aspects*, Springer-Verlag, New York.

Navon, A., Ittah, V., Landsman, P., Scheraga, H. A., and Haas, E. (2001) Distributions of intramolecular distances in the reduced and denatured states of bovine pancreatic ribonuclease A. Folding initiation structures in the C-terminal portions of the reduced protein, *Biochemistry 40*, 105-118.

Pletneva, E. V., Gray, H. B., and Winkler, J. R. (2005) Many faces of the unfolded state: Conformational heterogeneity in denatured yeast cytochrome c, *Journal of Molecular Biology 345*, 855-867.

Royer, C. A. (2006) Probing protein folding and conformational transitions with fluorescence, *Chemical Reviews 106*, 1769-1784.

Surrey, T., and Jahnig, F. (1992) Refolding and oriented insertion of a membrane-protein into a lipid bilayer, *Proceedings of the National Academy of Sciences of the United States of America 89*, 7457-7461.

Tamm, L. K., Arora, A., and Kleinschmidt, J. H. (2001) Structure and assembly of beta-barrel membrane proteins, *Journal of Biological Chemistry 276*, 32399-32402.

Wu, P. G., and Brand, L. (1994) Resonance energy transfer - methods and applications, *Analytical Biochemistry 218*, 1-13.